Journal of Ovonic Research Vol. 15, No. 4, July – August 2019, p. 239 - 246

SYNTHESIS AND PHOTOCATALYTIC PERFORMANCE OF g-C_3N_4 COMPOSITES

D. Y. LIU[a], J. H. DONG[b], F. M. LIU[a], X. F. GAO[a], Y. YU[a], S. B. ZHANG[a], L. M. DONG[a] , Y. K. GUO [a,*]
[a]*School of Materials Science and Engineering, Harbin University of Science and Technology, Harbin, China*
[b]*School of Chemical and Environmental Engineering, Harbin University of Science and Technology, Harbin, China*

Photocatalytic energy has been widely considered to be an effective solution to the problem of wastewater degradation. In this paper, g-C_3N_4 with different holding time was prepared by high temperature calcination, and the best catalytic results in different holding time were obtained by comparison test. Combined with the advantages of g-C_3N_4 and CuS, CuS/g-C_3N_4 composites with different g-C_3N_4 doping amount were prepared by water bath method. The structure and properties of the samples were characterized by X-ray diffraction, UV diffuse reflectance and fluorescence spectroscopy. Also, the methyl orange was used as the target pollutant. And the adsorption and photocatalytic efficiency of the composites were compared. Finally, CuS/g-C_3N_4 composite photocatalytic material with the best catalytic effect was obtained. Results showed: Different holding time had little effect on the photocatalytic effect, and the photocatalytic effect of carbon nitride with the holding time of 2 h was the best. Undoubtedly, the photocatalytic performance of the composites is much higher than that of g-C_3N_4 monomers. And the 9% CuS/g-C_3N_4 composite has the best photocatalytic performance and the highest degradation rate of methyl orange is up to 43.55%.

(Received April 19, 2019; Accepted August 7, 2019)

Keywords: Photocatalytic, CuS/g-C_3N_4, Composite material, Methyl orange

1. Introduction

In recent years, environmental pollution is a serious problem that needs to be solved in the world. More specifically, water pollution has seriously affected the ecological environment and human health, which has caused widespread concern. In particular, photocatalytic technology is a technology that converts solar energy into other energy sources. And it can also use solar energy to oxidize and degrade organic pollutants at room temperature [1], which is one of the most effective means to solve environmental pollution and energy shortage problems. The key to photocatalytic technology is to design and prepare catalysts that use sunlight efficiently [2].

However, the photocatalytic materials currently used in the industry still have certain defects in performance, and the utilization of light is not enough. More importantly, although metal oxide semiconductors can be used as photocatalytic materials, their photocatalytic efficiency is far below the level of industrial and domestic applications. More seriously, common photocatalysts, such as TiO_2, ZnO, Fe_2O_3, or other oxide-based species, show low or no catalytic activity in the absence of light, which greatly hinders their practical applicability for the continuous, around-theclock degradation of organic pollutants [3-8].Therefore, the development and establishment of efficient, harmless and sustainable semiconductor photocatalysts, using solar energy for photochemical degradation, can effectively solve the environmental crisis in the 21st century.

In 2009, Wang [9] et al. reported for the first time in Nature Materials that g-C_3N_4 has visible

*Corresponding author: 114668499@qq.com

light photocatalytic activity and is capable of photolysis of water to produce hydrogen under visible light. g-C_3N_4 has excellent band gap (2.7 eV), suitable band position and low cost and easy synthesis [10]. And it has been widely studied in the fields of photocatalytic hydrogen production, photocatalytic carbon sequestration and photocatalytic degradation of organic pollutants [11-14]. However, the layered g-C_3N_4 has a small specific surface area, fewer electrochemical reaction sites, and poor conductivity of g-C_3N_4, resulting in high recombination efficiency of photogenerated electrons and holes, which limits its in the field of photocatalysis Applications. Many efforts have been made to solve these problems. For example [15], forming a heterojunction semiconductor between g-C_3N_4 with an organic or inorganic substance to adjust the band gap, and doping metal/nonmetal or carbon materials were tried to improve visible light absorption and nanomaterials of photoelectron migration. Similarly, both organic dye or quantum dot sensitization and morphological design contribute to be improved light utilization efficiency and quantum yield of g-C_3N_4. However, g-C_3N_4 still lacks the assistance to utilize broad spectrum, even near-infrared light.

The metal sulfide and sulfide solid solution have a suitable band gap and can respond to sunlight and make a good photocatalyst. Noting that CuS is not only a good co-photocatalyst, but also a type of catalyst that can effectively degrade a wide range of organic pollutants with the help of hydrogen peroxide (H_2O_2) with or without light [16-17]. In this paper, the photocatalytic properties of g-C_3N_4 and CuS were combined to prepare CuS/ g-C_3N_4 catalysts, and their catalysts were tested. The best ratio of photocatalytic performance was compared with g-C_3N_4. The photocatalytic properties of the monomers were compared and conclusions were drawn.

2. Experimental section

2.1. Materials

Melamine ($C_3N_3(NH_2)_3$, AR), Tianjin Hengxing Chemical Reagent Manufacturing Co., Ltd; copper chloride ($CuCl_2$, AR), Tianjin Zhiyuan Chemical Reagent Co., Ltd; thioacetamide (CH_3CSNH_2, AR), Tianjin Tianli Chemical Reagent Co., Ltd; sodium dodecylbenzene sulfonate ($C_{18}H_{29}NaO_3S$, AR), Tianjin Hengxing Chemical Reagent Manufacturing Co., Ltd; methyl orange ($C_{14}H_{14}N_3SO_3Na$, AR), Tianjin Hengxing Chemical Reagent Manufacturing Co., Ltd.

2.2. Preparation of the g-C_3N_4

The g-C_3N_4 powders were prepared by melamine calcinating at high temperature. Typically, 9 g of melamine was put into the alumina crucible with the cover under the air atmosphere, heated to 500 °C with a heating rate of 10 °C/min and keep for 2 h. After cooling, g-C_3N_4 was lapped into powders and divided into three groups. Analogously, three sets of samples were placed in three crucibles with the half cover to heat to 520 °C at a heating rate of 5 °C/min. The holding time was 1 h, 2 h, and 5 h to complete the reaction, respectively,. After cooling to room temperature, the samples were lapped into a fine yellow powder to obtain three sets of g-C_3N_4 photocatalytic materials.

2.3. Preparation of the CuS/g-C_3N_4

CuS/g-C_3N_4 composites with different mass raions of g-C_3N_4 (5%, 9.5% and 29.5%,) were prepared through water bath method.Generally, 10.23 g $CuCl_2$•$2H_2O$ and 0.25 g sodium dodecylbenzenesulfonate (SDBS) were dissolved into 150 mL deionized water, and then the solution was placed on a magnetic stirrer to stirring well, named solution A. Solution A was divided into three equal portions, and 0.1 g, 0.2 g, 0.8 g of as-kept heated for 2 h g-C_3N_4 powders were added under a magnetic stirrer.

Then, 4.5 g of thioacetamide (TAA) was dissolved into 150 mL deionized water and named solution B, whcich was divided into three equal parts. The B solution was added to three parts of A solution under the action of a magnetic stirrer, where in the content of g-C_3N_4 was 5%, 9.5%, and 29.5%, respectively. Three sample solutions were placed in an conical flask, sealed with

plastic wrap, and placed in a water bath at 100 °C and keep for 4 h. Take out the conical flask and cool to room temperature. Then, the samples in the Erlenmeyer flask were put into centrifuge tubes and washed three times, washed twice with deionized water, and washed with absolute ethanol for the third time. The washed sample was dried in a drying oven at 80 °C for 4 h to obtain a CuS/g-C_3N_4 composite.

2.4. Characterization

The samples were characterized by different analytic techniques. Room temperature Powder X-ray diffraction (XRD) patterns of the samples were recorded using an X'Pert-ProMPD (Holand) D/max-γA X-ray diffractometer with Cu Kα radiation (λ=0.154178 nm). Scanning electron microscopy (SEM) images f the g-C_3N_4 precursor microsphereswere obtained with a SU8020 microscope with an accelerating voltage of 20 kV. UV-Vis absorption spectra were recorded on a 20 Lambda 750 (PerkingElmer) spectrophotometer in the wavelength range of 200-800 nm. The photoluminescence (PL) study was carried out on a Fluorolog-TCSPC Luminescence Spectrometer.

2.5. Photocatalytic performance study

Briefly, 0.1g photocatalyst was suspended in a 100 mL aqueous solution of 10 mg/L methyl orange.The solution was stirred for 1 h in the dark to ensure the establishment of adsorption equilibrium. Then,visible-light (300 W, xenon lamp) was obtained using cut-off filters to remove light of λ<420 nm. After every half an hour, 3.5 mL aliquots were extracted, centrifuged in the reaction process, and then analyzed using a UV-vis spectrophotometer at the maximum absorbed wavelength of 465 nm.

3. Results and discussion

3.1. Synthesis and charaterization of g-C_3N_4

Fig. 1 shows the XRD spectrum of the prepared g-C_3N_4.For g-C_3N_4, two pronounced peaks at 13.1° and 28.33° are found, which are in good agreement with graphitic phase carbon nitride [18]. The lower angle diffraction peak at 13.1° corresponds to tri-s-triazine units (100), and the other stronger one at 27.3° is derived from the interlayer stacking of aromatic segments (002). The test results show that the higher diffraction peak deviates contrast standard JCPDS 87-1526 card by 0.93°.

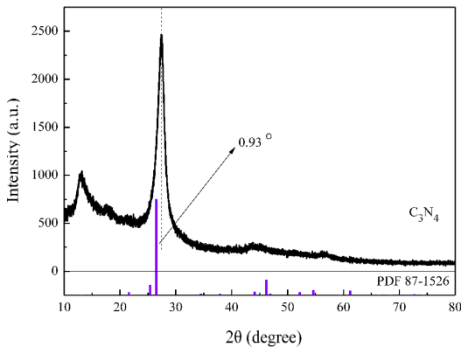

Fig. 1. XRD spectrum of g-C_3N_4.

Fig. 2 is a scanning electron micrograph of the prepared g-C_3N_4.The SEM of g-C_3N_4 shows that g-C_3N_4 is a lamellar structure with a stacking distribution causing fall off easily, and the size is about 5 μm.

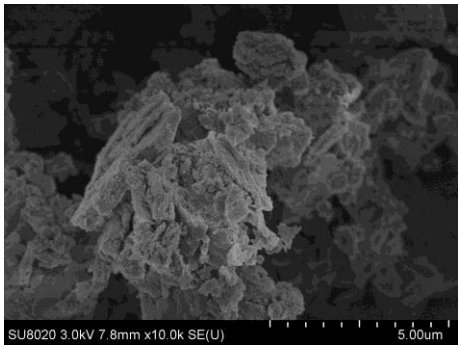

Fig. 2. SEM images of g-C_3N_4.

3.2. Synthesis and charaterization of CuS/g-C_3N_4

Fig. 3(a) shows the X-ray diffraction (XRD) patterns of the CuS/x%-g-C_3N_4 composites, where x is the weight ratio of g-C_3N_4 to CuS (5%, 9.5% and 29.5%,). The distinct peaks at 13.1° and 28.33° can be readily indexed as the (100) and (002) crystal planes of pure g-C_3N_4 ,and they appeared at all the CuS/g-C_3N_4 composites [19-20], which illustrated that the composite contained g-C_3N_4. In addition, the peak at 2θ=28.33° coincides with the diffraction peak of CuS. Notably, the diffraction peaks of the three groups of samples are shifted from the standard card(g-C_3N_4 JCPDS No. 87-1526, CuS JCPDS No. 75-2236), which possibly due to that the internal structure of CuS and g-C_3N_4 materials is changed after composited.

The strong peak at 2θ=33.33° is the diffraction peak of CuS in Fig. 3(b).Noticeably,the diffraction peaks corresponding to samples 1, 2 and 3 are all slightly offset. This could be attributed to g-C_3N_4 is introduced there in. For the CuS/ g-C_3N_4 composites with different g-C_3N_4 composites, the main characteristic peaks of CuS appeared entirely. It indicated that the composite was CuS/ g-C_3N_4.

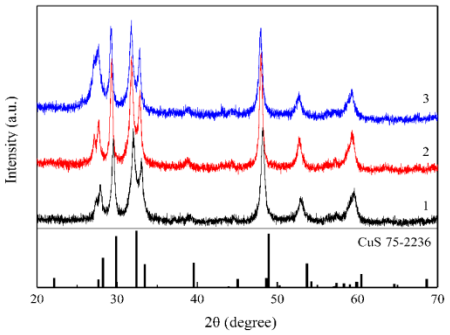

Fig. 3(a). XRD spectrum of CuS/g-C_3N_4 composite. (sample 1: 5%, sample 2: 9.5%, sample 3: 29.5%).

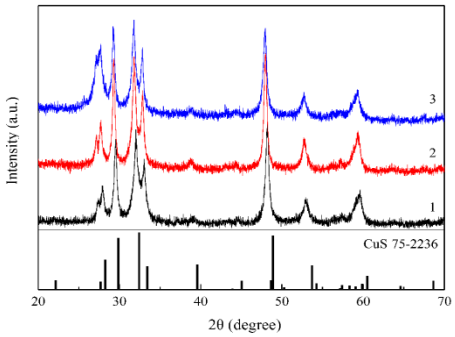

Fig. 3(b). Partial XRD spectrum of CuS/g-C_3N_4 composite.

3.3 Optical properties

The optical properties of samples was studied by the PL spectrum analysis and UV-vis absorption spectra. Photoluminescence (PL) spectra can reflect the charge transfer, capture and recombination of electron-hole pairs of photocatalytic materials. The high-strength photocatalytic material has a large amount of photogenerated carriers and good photocatalytic performance. Conversely, the photocatalytic material with low strength has less photogenerated carriers and poor photocatalytic performance. Ultraviolet absorption spectroscopy (DRS) can be used to characterize the change in the absorbance of a material,which can also be used to determine the absorption spectrum of a sample and to characterize it and structurally analyze it.

In Fig. 4, pure g-C_3N_4 shows a strong intrinsic fluorescence emission peak at 465 nm. According to the formula (1), the forbidden band width is calculated:

$$E_g = 1240 / \lambda_g \tag{1}$$

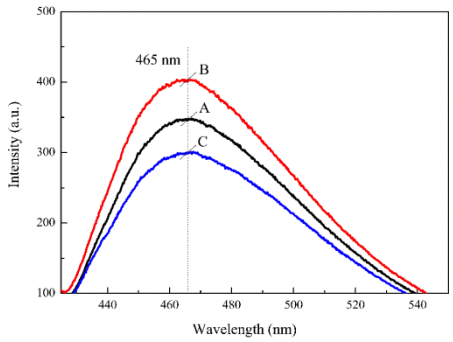

Fig. 4. Photoluminescence(PL) spectrum of g-C_3N_4.

Conseuently, the corresponding band gap energy (Eg) was calculated to about 2.66 eV. Additionally, the fluorescence intensity from high to low was followed by g-C_3N_4 samples with2 h, 1 h, and 5 h of heat preservation. The photocatalytic performance of the g-C_3N_4 sample with the heat preservation for 2 h is the best, and the photocatalytic performance of the sample with the thermal insulation for 1 h is the second. The photocatalytic performance of the g-C_3N_4 sample with the thermal insulation for 5 h is the worst. In this way, it is believed that the CuS/g-C_3N_4 photocatalytic composite material is better prepared by g-C_3N_4 sample with 2 h of heat preservation.

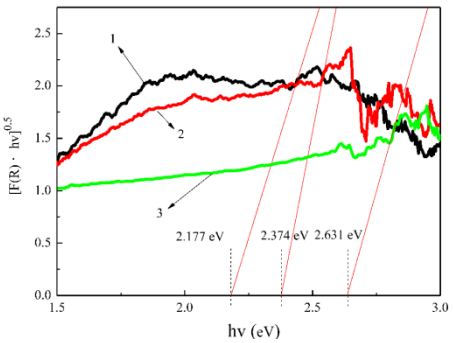

Fig. 5. DRS spectrum of CuS/g-C_3N_4 composite. (sample 1: 5%, sample 2: 9.5%, sample 3: 29.5%).

Fig. 5 shows that the ultraviolet diffuse reflectance (DRS) spectra of CuS/g-C_3N_4 composites with different g-C_3N_4 doping amounts. To get the forbidden band width, Selecting the first peak in the graph, then it was made a tangent, which was handed to the X-axis. According to the picture, the band gap energies of composite sample 1 , sample 2 and sample 3 were 2.177 eV, 2.374 eV, and 2.631 eV, separately. Smaller band gaps mean the lessenergy is required to induce efficient electron transfer. According to the data, the forbidden band width of the monomer g-C_3N_4 is 2.7 eV and the forbidden band width of the monomer CuS is 1.72 eV. So that the composite material was proved to be CuS/g-C_3N_4.

3.4. Photocatalytic performance analysis

Degradation performance of the sample is evaluated by decomposing methyl orange solution (MO). The decolorization rate of methyl orange degraded by g-C_3N_4 degradation of 10 mg/L was measured by a 722 visible spectrophotometer. And it was calculated by taking the methyl orange wavelength at 465 nm. The formula is as follows 2:

$$\left[(A_0 - A_*)/A_0\right] \bullet 100\% \tag{2}$$

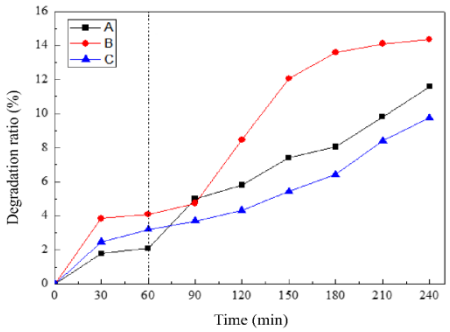

Fig. 6. Methyl orange degradation rate map. (A: 1 h incubation, B: 2 h incubation, C: 5 h incubation).

Fig. 6 shows a decolorization rate curve of g-C_3N_4 to methyl orange solution at different holding times. At the first 1 h, the Solution was made a dark treatment. the methyl orange adsorption rate of sample A ,the sample B and the sample C is 2.09%, 4.1%, 3.21%, respectively. After 3 h of light treatment, the decolorization rate of methyl orange in sample A, sample B and sample C was 11.59%, 14.36%, 9.75% , respectively. Based on the above analysis, we can safely conclude that the adsorption and photocatalytic effects of the g-C_3N_4 sample for 2 h were the best, which was consistent with the PL spectrum analysis results of g-C_3N_4 with different holding time. Therefore, the best choice is to composite g-C_3N_4 kept for 2h with CuS to improve photocatalytic efficiency.

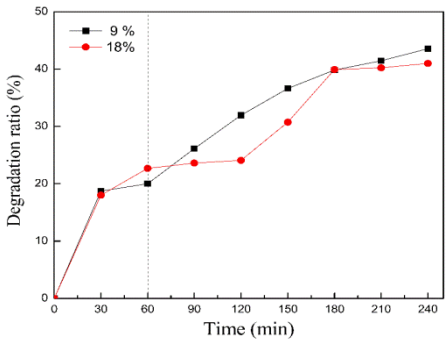

Fig. 7. Decolorization rate of methyl orange. (sample A: 5%, sample B: 9.5%).

Fig. 7 displays a comparison chart of decolorization ratio of methyl orange in CuS/g-C_3N_4 composite with different g-C_3N_4 doping amount. Under the conditions of laboratory simulated sunlight, different g-C_3N_4 doping amounts of CuS/g-C_3N_4 composites degraded methyl orange. Moreover, the CuS/g-C_3N_4 catalysts exhibited higher degradation activity than pure g-C_3N_4, which confirms that the interface between CuS and g-C_3N_4 could successfully suppress electron–hole recombination and improve the photocatalytic activity.At the first 1 h in the dark state, the adsorption efficiency of methyl orange in the CuS/g-C_3N_4 composite with different g-C_3N_4 doping amount was close to coincident in the first 30 minutes, which indicating that the different g-C_3N_4 doping has no significant effect on the adsorption of the composite. Furthermore, 9.5% doped composites have better adsorption effect after 30 minutes. Photocatalytic efficiency of methyl orange in CuS/g-C_3N_4 composites with different g-C_3N_4 doping contents were compared under natural light irradiation at 2-4 h. It was clear that 5% g-C_3N_4 doping the catalytic properties of the hybrid composites were significantly better than those of the 9.5% samples at 2-3 h. In addition, the latter had a significant upward trend and was close to the former at 3 h. but it tends to decrease after 3 h. Among the catalysts, the CuS/g-C_3N_4 composite with 5% g-C_3N_4 doping has better photocatalytic effect than the 9.5% composite.

4. Conclusions

CuS/g-C_3N_4 composites with CuS anchored on g-C_3N_4 sheets were successfully fabricated via asimple water bath method. UV–vis and PL spectroscopy indicatedthat the CuS/g-C_3N_4 composites have good visible light absorption and can efficiently transfer photoinduced electron–hole pairs at the interface between CuS and g-C_3N_4, which can improve its photocatalytic activity towards organic pollutants in sewage under visible light. The g-C_3N_4 samples with different incubation times have similar structures and are lamellar. Similar, there was no significant difference. However, it was found by PL spectroscopy and photocatalytic performance test that the photocatalytic performance of the g-C_3N_4 monomer sample with the heat preservation for 2 h was the best, and the photocatalytic performance of the sample with the thermal insulation for 5 h was the worst.

In addition, CuS/g-C_3N_4 composites with different compositions were found to have high degradation rate of methyl orange in CuS/g-C_3N_4 composites with 5% carbon nitride composite content in the three samples with different ratios. The composite materials of the other two groups of g-C_3N_4 composites reached 43.55 %. By comparison, the photocatalytic performance of the prepared CuS/ g-C_3N_4 composite material is greatly improved compared with the monomer g-C_3N_4. Moreover, the catalytic performance of g-C_3N_4 monomer is general when the holding time is short, but the catalytic property is lowered as the holding time is too long. Only the moderate holding time can get the best performance g-C_3N_4 monomer material.

Acknowledgment

This work was financially supported by Heilongjiang University Students Innovation and Entrepreneurship Project (201710214031).

References

[1] C. Zeng-Yong, Y. Bo, Y. Ting-Nan, Journal of Inorganic Materials, **29**(8), 785 (2014).
[2] H. Tada, Q. Jin, H. Nishijima, H. Yamamoto, M. Fujishima, S. Okuoka, H. Kobayashi, Angewandte Chemie International Edition **50**, 3501 (2011).
[3] C.-C. Wang, J.-R. Li, X.-L. Lv, Y.-Q. Zhang, G. Guo, Energy Environ. Sci. **7**, 2831–67 (2014).

[4] X. Li, J. Yu, M. Jaroniec, Chemical Society Reviews **45**, 2603 (2016).
[5] Y. Wang, H. Huang, J. Gao, G. Lu, Y. Zhao, Y. Xu, et al. Journal of Materials Chemistry A **2**, 12442 (2014).
[6] H. Yin, X. Chen, R. Hou, H. Zhu, S. Li, Y. Huo et al., ACS Applied Materials & Interfaces **7**, 20076 (2015).
[7] M. Sakar, C.-C. Nguyen, M.-H. Vu, T.-O. Do, ChemSusChem. **11**, 809 (2018).
[8] Y. Lu, X. Zhang, Y. Chu, H. Yu, M. Huo, J. Qu et al., Appllied Catalysis B-Environmental **224**, 239 (2018).
[9] X. Wang, K. Maeda, A. Thomas et al., Nature Material **8**, 76 (2009).
[10] Y. Wang, X. Wang M. Antonietti, Angewandte Chem-International Edition **51**, 68 (2012).
[11] R. Mo, J. Li, Y. Tang, H. Li, J. Zhong, Surface Science **15**, 552 (2019).
[12] X. She, J. Wu, J. Zhong, H. Xu, Y. Yang, R. Vajtai, P. M. Ajayan, Nano Energy **27**, 138 (2016).
[13] H. Wang, Z. Sun, Q. Li, Q. Tang, Z. Wu, Journal of CO_2 Utilization **14**, 143 (2016).
[14] Y. Ma, J. Zhang, Y. Wang, Q. Chen, Z. Feng, T. Sun, Advanced Research **16**, 135 (2018).
[15] J. Qin, H. Zeng, Catalysis B: Environmental **2009**, 161 (2017).
[16] C. Deng, X. Ge, H. Hu, L. Yao, C. Han, D. Zhao ,CrystEngComm, **16**, 2738 (2014).
[17] Q. Shu, J. Lan, M. Gao, J. Wang, C. Huang, CrystEngComm, **17**, 1374 (2015).
[18] F. Guo, W. Shi, W. Guan, H. Huang, Y. Liu, Purif. Technol, **173**, 295 (2017).
[19] G. Liao, S. Chen, X. Quan, H. Yu, H.Zhao, Materials Chemistry **22**, 2721 (2012).
[20] F. Dong, Z. Zhao, T. Xiong, Z. Ni, W. Zhang, Y. Sun, et al., ACS Appl Mater Interfaces **5**, 11392 (2013).